VIBRATIONAL DEPENDENCE OF LINE COUPLING AND LINE MIXING IN SELF-BROADENED PARALLEL BANDS OF NH_3

Q. Ma, C. Boulet, R.H. Tipping

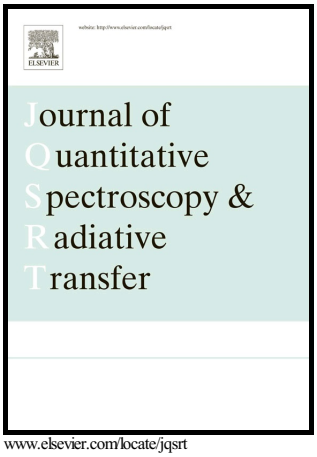

www.elsevier.com/locate/jqsrt

PII: S0022-4073(16)30819-6
DOI: http://dx.doi.org/10.1016/j.jqsrt.2017.01.010
Reference: JQSRT5557

To appear in: *Journal of Quantitative Spectroscopy and Radiative Transfer*

Received date: 2 December 2016
Revised date: 6 January 2017
Accepted date: 6 January 2017

Cite this article as: Q. Ma, C. Boulet and R.H. Tipping, VIBRATIONAL DEPENDENCE OF LINE COUPLING AND LINE MIXING IN SELF BROADENED PARALLEL BANDS OF NH_3, *Journal of Quantitativ Spectroscopy and Radiative Transfer*, http://dx.doi.org/10.1016/j.jqsrt.2017.01.010

VIBRATIONAL DEPENDENCE OF LINE COUPLING AND LINE MIXING IN SELF-BROADENED PARALLEL BANDS OF NH_3

Q. Ma[1], C. Boulet[2], R.H. Tipping[3]

[1]NASA/Goddard Institute for Space Studies and Department of Applied Physics and Applied Mathematics, Columbia University, 2880 Broadway, New York, New York 10025, USA

[2]Institut des Sciences Moléculaires d'Orsay (ISMO), CNRS, Univ. Paris-Sud, Université Paris-Saclay, Bât.350, Campus d'Orsay F-91405, France

[3]Department of Physics and Astronomy, University of Alabama, Tuscaloosa, AL 35487-0324, USA

Abstract

Line coupling and line mixing effects have been calculated for several self-broadened NH_3 lines in parallel bands involving an excited ν_2 mode. It is well known that once the ν_2 mode is excited, the inversion splitting quickly increases as this quantum number increases. In the present study, we have shown that the ν_2 dependence of the inversion splitting plays a dominant role in the calculated line-shape parameters. For the ν_2 band with a 36 cm^{-1} splitting, the intra-doublet couplings practically disappear and for the $2\nu_2$ and $2\nu_2$ - ν_2 bands with much higher splitting values, they are completely absent. With respect to the inter-doublet coupling, it becomes the most efficient coupling mechanism for the ν_2 band, but it is also completely absent for bands with higher ν_2 quantum numbers. Because line mixing is caused by line coupling, the above conclusions on line coupling are also applicable for line mixing. Concerning the check of our calculated line mixing effects, while the present formalism has well explained the line mixing signatures observed in the ν_1 band, there are large discrepancies between the measured Rosenkranz mixing parameters and our calculated results for the ν_2 and $2\nu_2$ bands. In order to clarify these discrepancies, we propose to make some new measurements. In addition, we have calculated self-broadened half-widths in the ν_2 and $2\nu_2$ bands and made comparisons with several measurements and with the values listed in HITRAN 2012. In general, the agreements with measurements are very good. In contrast, the agreement with HITRAN 2012 is poor, indicating that the empirical formula used to predict the HITRAN 2012 data has to be updated.

1. INTRODUCTION

Accurate laboratory data on the spectral line parameters for NH_3 are required for planetary atmosphere remote sensing. In order to meet this requirement, several authors have reported self-broadening coefficients of NH_3 lines in various vibrational bands during the past few years. Beside the ν_1 and pure rotational bands [1,2] studied by the current authors in Refs. [3,4] (denoted as papers I and II in the following), a number of

measurements have also been published for other parallel bands. Baldacchini et al. have measured half-widths in the ν_2 and $2\nu_2$ - ν_2 bands [5-7] and their results were compared with predictions of the Anderson-Tsao-Curnutte (ATC) theory [8]. In 2004, Nemtchinov et al. [9] have made a systematic study of pressure broadening in the 10 µm bands of NH_3, including the ν_2 band. At the same time, Aroui et al. [10] have measured self-broadening coefficients in the ν_2 band and, more recently [11], they have published a more complete study of the 10 µm spectral region. By using a non-linear least-squares fitting procedure, they have simultaneously determined not only the half-widths in the ν_2 and $2\nu_2$ bands, but also the Rosenkranz line mixing parameters Y_l. More recently, half-widths of lines with high j and k values in the R branch of the ν_2 band have been measured by Guinet et al. [12].

In papers I and II, we have demonstrated the need to take into account the inversion splitting in half-widths calculations in the ν_1 and pure rotational bands. More precisely, we have shown that, in general, the intra-doublet coupling plays a major role in the reduction of calculated half-widths (i.e., the diagonal elements of the relaxation matrix). Such reductions by large amounts indicate significant off-diagonal elements of the relaxation matrix. Indeed, the whole relaxation matrices calculated by us with our new formalism have demonstrated their non-diagonality. The method has been successfully applied to the calculation of the shape of the Q branch and of some R manifolds in the ν_1 band, for which an obvious signature of line mixing (LM) caused by this non-diagonality had been experimentally demonstrated [1].

As shown in I and II, the main parameter governing the importance of line coupling (LC) within doublets is the inversion splitting. Meanwhile, it is well known that the latter largly varies with the vibrational states of interest. For example, while it is about 0.8 cm^{-1} in the ground and $\nu_1 = 1$ vibrational states, it increases to 35 cm^{-1} and 284 cm^{-1} for the $\nu_2 = 1$ and $\nu_2 = 2$ states, respectively. Based on experiences learnt from papers I and II, we expect that, in comparisons with the ν_1 and pure rotational bands, LC (and hence LM) should be much smaller in the ν_2 band and itbecomes completely negligible in the $2\nu_2$ band. Therefore, it is worth to complete our previous studies by considering more parallel bands of NH_3 where measured data are available. In addition, this would enable to analyze the vibrational dependence of both self-broadening coefficients and line mixing parameters.

The manuscript is arranged in the following way. Section 2 gives a brief summary of the theoretical model. Sec. 3 is devoted to comparisons of calculated and experimental half-widths, to an analysis of the role of the vibrational dependence of the inversion splitting on the efficiency of the LC process and to comparison with the broadening coefficients given by the HITRAN 2012 database. Finally we complete this study by examining the vibrational dependence of the relaxation matrix and of the line mixing parameters in sec. 4. The disagreement between some experimental and calculated line mixing parameters is discussed and some experiments are suggested in order to clarify this discrepancy.

2. THEORY

In this section, we briefly outline the main features of the formalism developed in papers I and II. In these two papers and other earlier works [13] devoted to the line coupling, we have pointed out that, in order to avoid the cut-off introduced in the ATC theory, the authors of the Robert-Bonamy (RB) formalism [14] had applied the linked cluster theorem to evaluate the Liouville scattering operator $\hat{S}$. However, they had neglected the non-diagonality of the $\hat{S}$ operator. Unfortunately, the applicability of this so-called isolated line approximation is not valid in many cases so that relying on this assumption is one of the main weaknesses of the RB formalism.

In our recent works, we have proposed a new formalism by correctly applying the cumulant expansion to evaluate the Liouville scattering operator $\hat{S}$ up to the second order terms (S_1 and S_2). In contrast with the RB formalism or the model developed by Cherkasov [15,16], the S_1 and S_2 terms defined in our formalism are independent of the bath molecular states. This enables to diagonalize the operator $-iS_1 - S_2$ and consequently to evaluate the whole matrix elements of $\exp(-iS_1 - S_2)$. As a result, the introduction of the so-called isolated line approximation becomes completely unnecessary. In papers I and II, we have presented general expressions of the matrix elements of S_1, $S_{2,outer,i}$, $S_{2,outer,f}$ and $S_{2,middle}$ for parallel bands of NH_3. It is well known that in general, the non diagonality of $-iS_1 - S_2$ solely results from the $S_{2,middle}$ term. The expression for its matrix elements in a symmetrized formalism are given by (cf. Eq. (11) of paper I)

$$\begin{aligned} S_{2,middle}^{i'f',if}(r_c) &= 2\pi\,(-1)^{1+J}\delta_{\nu_i'\nu_i}\delta_{\nu_f\nu_f'}(-1)^{j_f+j_f'} \\ &\times\sqrt{(2j_i'+1)(2j_f'+1)(2j_i+1)(2j_f+1)}\sum_{L_1K_1K_1'L_2K_2K_2'}(-1)^{L_1}W\left(j_i'j_f'j_ij_f,JL_1\right) \\ &\times D^P(\varepsilon_i'j_i'k_i',\varepsilon_ij_ik_i;L_1K_1)D^P\left(\varepsilon_fj_fk_f,\varepsilon_f'j_f'k_f';L_1K_1'\right) \\ &\times\sum_{i_2i_2'}\sqrt{\rho_{i_2}\rho_{i_2'}}(2j_2+1)(2j_2'+1) \\ &\times D^P(\varepsilon_2'j_2'k_2',\varepsilon_2j_2k_2;L_2K_2)D^P(\varepsilon_2j_2k_2,\varepsilon_2'j_2'k_2';L_2K_2') \\ &\times\ \mathbb{F}_{L_1K_1K_1'L_2K_2K_2'}\left(\frac{\omega_{i'i}+\omega_{f'f}}{2}+\omega_{i_2'i_2},\omega_{fi}-\omega_{f'i'}\right), \end{aligned} \tag{1}$$

where all symbols have been defined in paper I.

As shown in Eq. (1), the magnitudes of the off-diagonal element of $S_{2,middle}$ depend on three factors. The first one is the coupling strength factor defined by

$$\begin{aligned} &(-1)^{L_1}\sqrt{(2j_i'+1)(2j_f'+1)(2j_i+1)(2j_f+1)}\,W\left(j_i'j_f'j_ij_f,JL_1\right) \\ &\times D^P(\varepsilon_i'j_i'k_i',\varepsilon_ij_ik_i;L_1K_1)D^P\left(\varepsilon_fj_fk_f,\varepsilon_f'j_f'k_f';L_1K_1'\right). \end{aligned} \tag{2}$$

The others are the two arguments of the two dimensional (2-D) Fourier transforms $\mathbb{F}_{L_1K_1K_1'L_2K_2K_2'}$ with specified L_1, K_1, and K_1': the energy gap $\frac{\omega_{i'i}+\omega_{f'f}}{2}+\omega_{i_2'i_2}$ and the frequency gap $\omega_{fi}-\omega_{f'i'}$. The energy gap represents the resonant character (in the sense of the ATC-RB formalisms) of the two coupled lines and the frequency gap is their separation in the spectrum. As shown in paper I, beyond their central regions, the magnitudes of $\mathbb{F}_{L_1K_1K_1'L_2K_2K_2'}$ decrease very quickly as their two arguments increase. This variation pattern indicates that the smaller these two gaps are, the stronger the LC.

For later convenience, we introduce a notation of $W^{(b)}_{L_2K_2K_2'}(i_2i_2')$ defined by

$$W^{(b)}_{L_2K_2K_2'}(i_2i_2') = \sqrt{\rho_{i_2}\rho_{i_2'}}(2j_2+1)(2j_2'+1) \times D^P(\varepsilon_2'j_2'k_2', \varepsilon_2 j_2 k_2; L_2K_2)D^P(\varepsilon_2 j_2 k_2, \varepsilon_2'j_2'k_2'; L_2K_2'), \quad (3)$$

whose value divided by $(2L_2+1)$ is a probability with which a specified perturber frequency change of $\omega_{i_2'i_2}$ appears in $\mathbb{F}_{L_1K_1K_1'L_2K_2K_2'}$ of Eq. (1).

Once all matrix elements of $\exp(-iS_1-S_2)$ have been obtained, it is easy to calculate the relaxation matrix elements using the following expression [3,4]

$$\widetilde{W}_{i'f',if} = \frac{n_b\bar{v}}{2\pi c}\int_{r_{c,min}}^{+\infty} 2\pi(b\frac{db}{dr_c})dr_c\{\delta_{i'i}\delta_{f'f} - \ll i'f'\left|e^{-iS_1(r_c)-S_2(r_c)}\right|if \gg\}, \quad (4)$$

where n_b is the number density of the bath molecules, $\bar{v}$ is the mean relative speed, b is the impact parameter, and r_c is the closest distance for a given trajectory.

3. PRACTICAL CALCULATIONS

3.1. Potential model

The intermolecular potential has been detailed in sec. II-C of paper I. With respect to its isotropic part, it is represented by a LJ model. By neglecting their vibrational dependence, the two LJ parameters (i.e., σ_{LJ} = 3.018 Å and ε_{LJ} = 294.3 K) adopted here are the same as those used in Paper I.

Because the NH_3 molecule has a very large dipole moment and a significant quadrupole moment, the anisotropic interaction between two NH_3 molecules can be well represented by a summation of the dipole-dipole (V_{dd}), dipole-quadrupole (V_{dq}), quadrupole-dipole (V_{qd}), and quadrupole-quadrupole (V_{qq}) components. It is obvious that among these components, V_{dd} is the dominant one.

Table 1 Vibrational dependence of the averaged dipole moment (in Debye)

Vibrational state	Ground	ν_1	ν_2	$2\nu_2$
$\langle v\|\mu\|v\rangle$	1.4483	1.47925	1.24495	1.01535

It is worth mentioning that values of the dipole moment appearing in the expressions for the S_2 terms are average dipole moments $\langle v|\mu|v\rangle$ in the corresponding vibrational states. The values used in the present study, given in Table 1 [17], show that the average dipole values exhibit a significant vibrational dependence which may affect the calculation of the S_2 matrix elements. Remember that the contributions to the three S_2 terms from V_{dd} are proportional to the products of two dipole values. For example, the magnitude of the $S_{2,outer,f}$ term is proportional to $\langle v_f|\mu|v_f\rangle^2$.

3.2. Rovibrational energy levels of NH_3

As explained in paper I, the present formalism, which uses "0-th" order wavefunctions, does not consider the various intra-molecular couplings that exist between the NH_3 levels. The same approximation allows a simple calculation of the energy levels with two sets of

parameters associated with the symmetric and asymmetric inversion levels. The energy parameters are given in Table 6a and the formulas for the energies in Table 4 (diagonal elements) of Ref. [18]. Numerical tests have demonstrated the validity of this approximation for states whose rotational quantum numbers are not too high.

3.3. Construction of the linespace

Because the dipole and quadrupole moments of NH_3 lie along its symmetry axis, the matrix elements of the anisotropic potential between two rotational states are zero unless their k values are identical. This implies that the coupling selection rules is $\Delta k = 0$, which coincides with the radiative dipolar selection rule for parallel bands. Consequently, the whole linespace can be divided into uncoupled sub-blocks constructed for lines with specified k values. In the present study, we limit the size of the linespace by only considering lines with initial angular quantum number j up to $j_{max} = 8$. With this limitation, the whole linespace involves 217 Lines and it is divided into 9 sub-blocks associated with k = 0, 1, 2, …, 8, respectively. For example, there are 17 lines whose k values is zero, the dimension of the sub-block with k = 0 is 17×17. Similarly, one can easily determine the dimensions of other sub-blocks as 46 x 46, 40 x 40, 36 x 36, 28 x 28, 22 x 22, 16 x 16, 10 x 10 and 4 x 4.

3.4. Trajectory model

The “exact” trajectory model governed by the isotropic part of the intermolecular potential is used in calculations. As done in papers I and II, 600 values of the closest approach distance r_c have been selected in order to represent all the accessible trajectories, with a more dense grid for nearly head-on collisions. As shown in Eq. (4), calculations have been restricted to the average relative kinetic energy $\bar{E}_{kin} = \frac{4k_BT}{\pi}$ associated to the mean velocity at temperature T. Such an approximation is known to be valid for self-broadening coefficients calculations. For the off-diagonal elements of W, we expect that the uncertainty associated with neglecting the velocity average is tolerable. A more refined treatment in which we take into account the kinetic energy dependence of the relaxation matrix is under way.

4. RESULTS OF CALCULATED HALF-WIDTHS

4.1. Comparison with experimental data

Calculated half-widths of lines in the ν_2 band are compared with experimental results in Figs. 1-3. In general, the calculated valuess (including a weak LC effect that will be discussed later on) agree well with the experimental data. A large disagreement is obtained for one single transition, sP(2,1), between the measurement by Nemtchinov et al. [9] (290.3×10^{-3} $cm^{-1}\,atm^{-1}$) and our calculated value ($470.8 \times 10^{-3}\,cm^{-1}\,atm^{-1}$) as shown in Fig. 2. However, a recent analysis of old Kitt Peak spectra [19] gave a new result of $445 \times 10^{-3}\,cm^{-1}\,atm^{-1}$ with ± 8% uncertainty, in good agreement with our theoretical value.

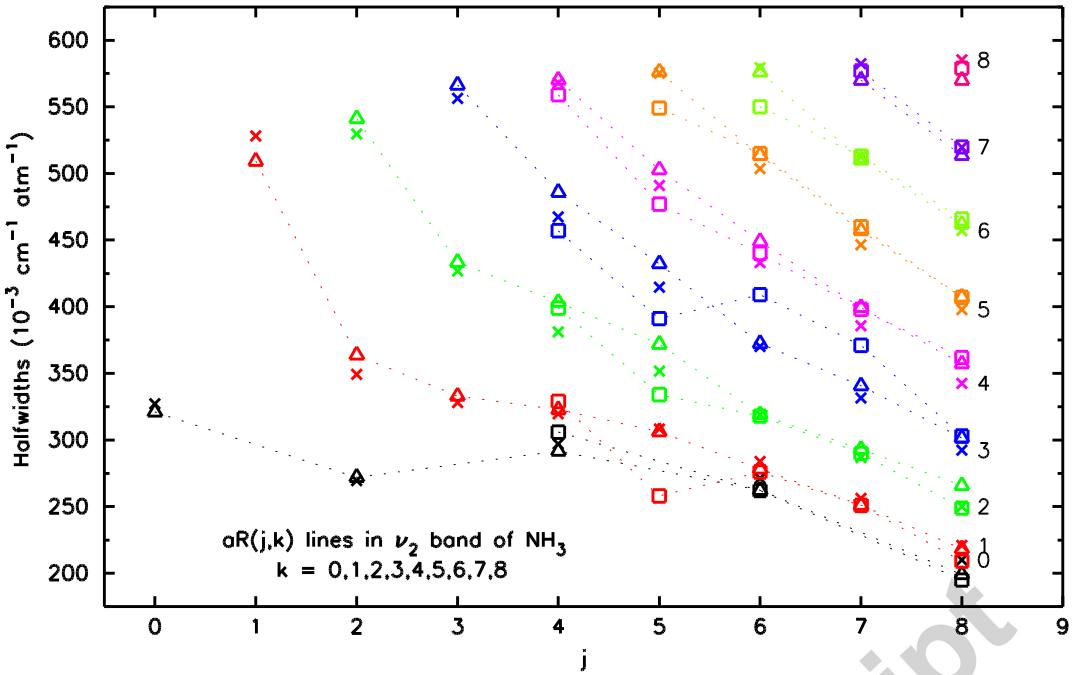

Fig. 1. Comparison of calculated half-widths **(×)** of aR(j,k) lines in the ν_2 band with measurements (Δ) by Nemtchinov et al. [9] and (□) by by Aroui et al. [11]. The values of k are presented at the right side of symbols representing calculated values with j = 8 and different colors are used to distinguish different k values. In addition, measured results with the same k values are connected by dotted thin lines.

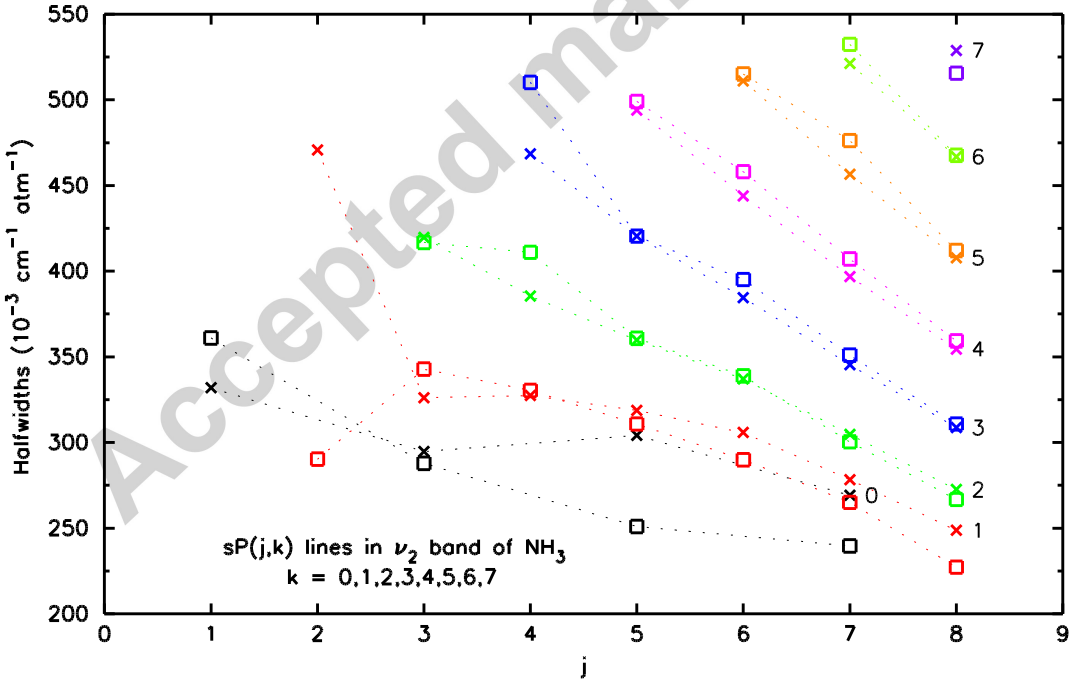

Fig. 2. Comparison of calculated half-widths **(×)** for sP(j,k) lines in the ν_2 band with those **(□)** measured by Nemtchinov et al. [9]. The large difference observed for sP(2,1) is discussed in the text.

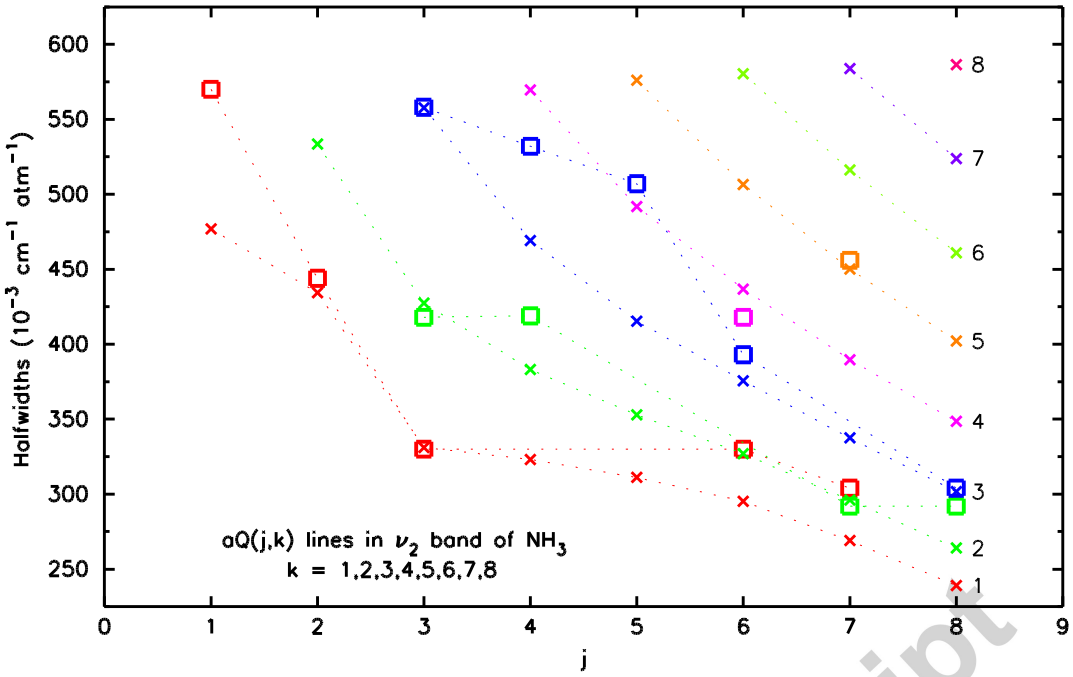

Fig. 3. Comparison of calculated half-widths **(×)** for aQ(j,k) lines in the ν_2 band with measured data **(□)** of Ref. |5]. The experimental uncertainty is around ±10%.

Calculated half-widths of lines in the $2\nu_2$ band are compared with experimental results provided by Aroui et al. [11] in Fig. 4, showing a very good agreement. Meanwhile, a comparison between measurements by Baldacchini et al. [6,7] and our calculated values for lines in the $2\nu_2$ - ν_2 band is presented in Table 2. Given the fact that the experimental results have a ±10 % uncertainty, the agreement is excellent. Finally, we note that the important vibrational dependence of the widths is well predicted by the formalism. We will go back to this issue later.

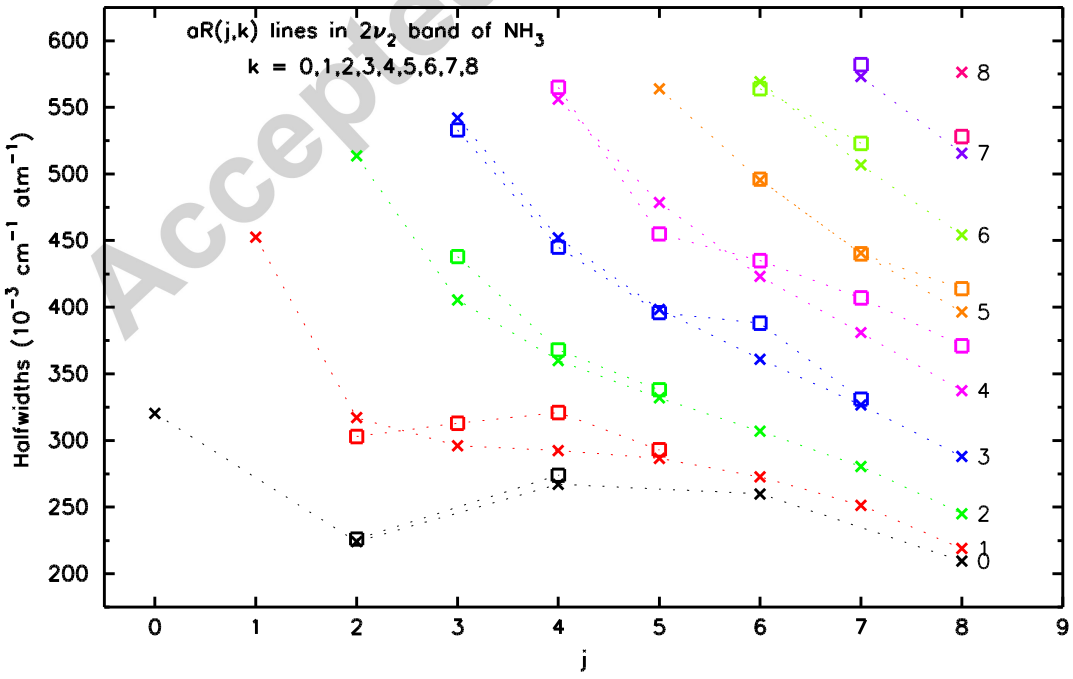

Fig. 4. AComparison between calculated half-widths **(×)** for aR(j,k) lines in the $2\nu_2$ band and those **(□)** measured by Aroui et al. [11].

Table 2 Half-widths (in units of 10^{-3} cm^{-1} atm^{-1}) for sQ(j,k) lines in $2\nu_2$ - ν_2 band

j, k	Experiment Ref. [6]	Calculated values
1, 1	241	246.3
2, 2	266	249.6
3, 3	254	247.2
4, 3	254	237.4
4, 4	266	245.1
5, 3	228	239.0
6, 3	228	240.8
6, 6	228	238.3
7, 6	228	238.2
8, 7	228	233.7
8, 8	228	229.5

4.2. Reduction of calculated half-widths due to the line coupling

In Figs. 5. and 6. we present relative differences between half-widths derived with and without considering LC. As can be seen, the reductions of calculated half-widths by LC are weak when compared with those in both the ν_1 and the pure rotational bands (compare with Fig. 5. of paper I). Given the fact that when the ν_2 mode is excited a huge increase of the inversion splitting occurs, this trend is expected.

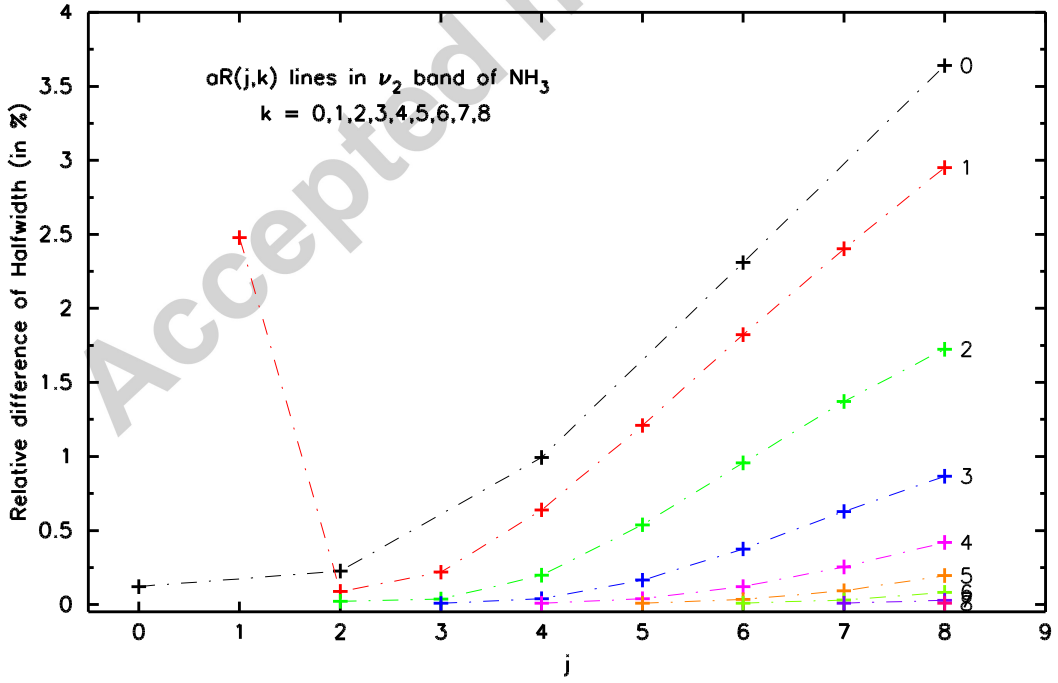

Fig. 5. Relative differences between half-widths (i.e., $[\gamma_{noLC} - \gamma_{LC}]/\gamma_{LC}$) calculated with and without considering LC for aR(j,k) lines in the ν_2 band.

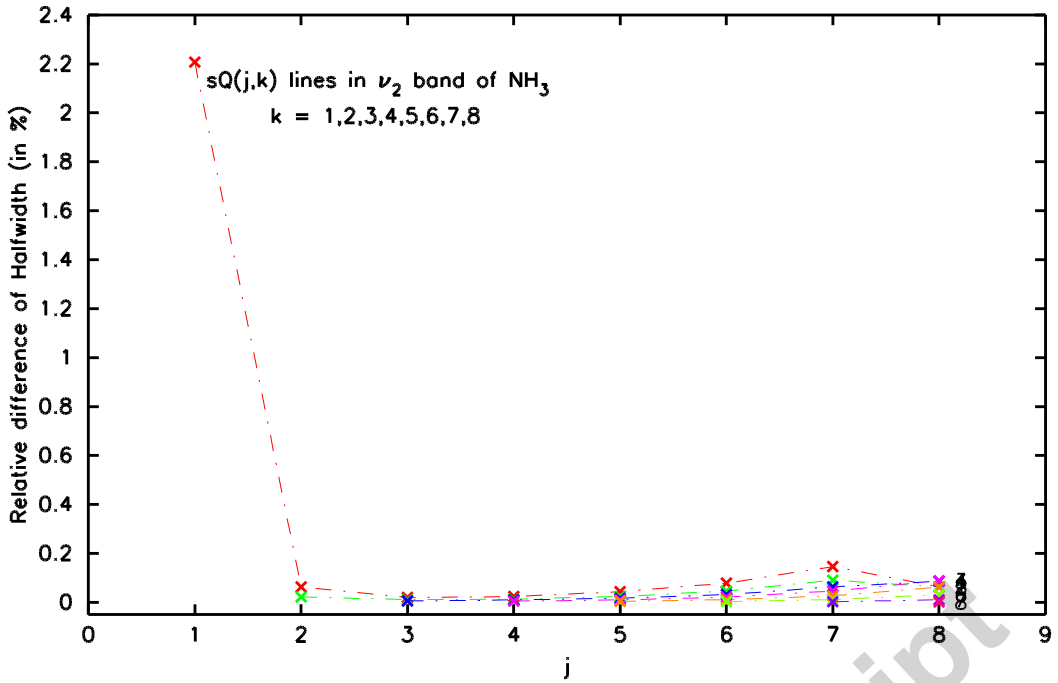

Fig. 6. The same as Fig. 5. except for the sQ(j,k) lines. The large reduction for the sQ(1,1) line results from its strong coupling with the aR(1,1) line.

The "anomalous" large reductions happening for aR(1,1) and sQ(1,1) in Figs. 5 and 6, respectively, deserve an explanation. They result from the same origin, i.e., a relatively small but significant coupling between aR(1,1) and sQ(1,1) which is allowed by the dipole selection rule. Their frequency gap (i.e., 1.9 cm^{-1}) is rather small. With respect to their energy gap $(\omega_{i'i} + \omega_{f'f})/2 + \omega_{i_2'i_2}$, its first component $\omega_{i'i}/2$ can be neglected since it is equal to one half of the inversion splitting (i.e., 0.8 cm^{-1}) in the ground state. Meanwhile, the values of $\omega_{f'f}$ can be estimated by a simple formula

$$\omega_{f'f} \cong \pm\,\delta_{sa}^{\nu_2} + B\left[j_f'\left(j_f'+1\right) - j_f\left(j_f+1\right)\right], \qquad (5)$$

where $\delta_{sa}^{\nu_2}$ is the inversion splitting, the plus and minus signs are for transitions of a ← s and s ← a, respectively, and the rotational constant is B ≅ 10 cm^{-1}. With Eq. (5), the second component $\omega_{f'f}/2$ can be approximated by $(\delta_{sa}^{\nu_2} - 40)/2$. The inversion splitting in the ν_2 = 1 band is $\delta_{sa}^{\nu_2} \cong 36$ cm^{-1} and consequently, the of $\omega_{f'f}/2$ (i.e., –2 cm^{-1}) is small.

For the third component $\omega_{i_2'i_2}$ associated with the bath molecule, we plot a distribution of $W_{100}^{(b)}(i_2 i_2')$ in Fig. 7. Its intensities divided by 3 represent probabilities with which specified values of $\omega_{i_2'i_2}$ occur. We note that the resolution adopted here is 0.5 cm^{-1}. In other words, the values within [ω_0 – 0.25, ω_0 + 0.25] are grouped to its total value at ω_0. As clearly demonstrated in the plot, the occurring of $\omega_{i_2'i_2} \cong 0$ is dominant. Therefore, in order to simplify the analyses, one can neglect it.

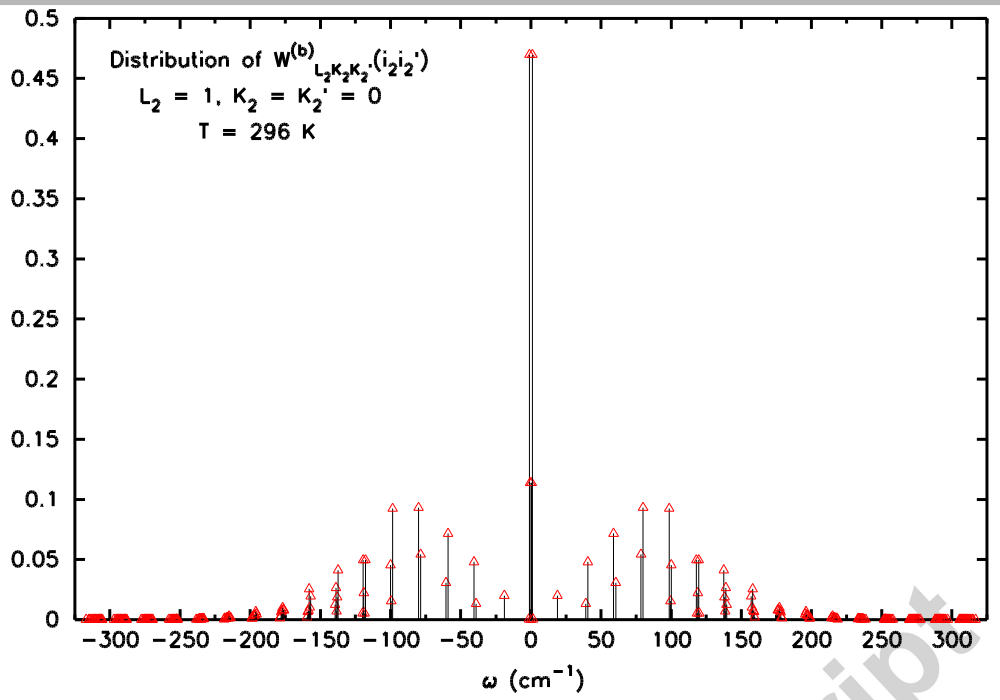

Fig. 7. The distribution of $W^{(b)}_{L_2K_2K_2'}(i_2 i_2')$ over $\omega_{i_2' i_2}$ with a resolution of 0.5 cm^{-1}. After dividing by $(2L_2 + 1)$, the values represent the probability with which $\omega_{i_2' i_2}$ appears as the third component of the energy gap.

Thus, based on the above discussion, one can conclude that because their energy gap is more likely small, many significant contributions to the off-diagonal elements of $S_{2,middle}$ exist for this pair and consequently, "anomalous" reductions happen for these two lines. We will go back to the aR(1,1) line in the section devoted to LM effect.

4.3. Intra- and Inter-doublet couplings

For doublet partners, their frequency gap is given by the doublet splitting. For the ν_1 and pure rotational bands, it is about 0.8 cm^{-1} and leads to large magnitudes of the 2-D Fourier transforms. As a result, for these two bands, the intra-doublet coupling is the main source responsible for the line coupling. For the ν_2 band which has a splitting of about 36 cm^{-1}, there is a different story. With such a large gap, the magnitudes of 2-D Fourier transforms fall down to a negligible level (see the discussion around Fig. 3. of paper I). This implies that the intra-doublet coupling practically disappears for the ν_2 band and becomes completely absent for the $2\nu_2$ and $2\nu_2$ - ν_2 bands. (Remember that the inversion splitting is about 284 cm^{-1} in the $\nu_2 = 2$ level).

For the ν_2 band, the inter-doublet coupling becomes the most efficient coupling mechanism. More explicitly, the coupling mainly takes place between two lines belonging to adjacent doublets whose j values differ by 1. An example is the inter-doublet coupling between sR(j,k) and aR(j+1,k) allowed by the dipole selection rule. In Fig. 8, we present the frequency gap between these pairs as a function of j and k. By comparing Figs. 5 and 8, a perfect correlation is clearly seen. Then, one can draw two conclusions. Firstly, the inter-

doublet coupling is actually the dominant coupling mechanism. Secondly, it is the frequency gap that plays a major role in the j and k dependence of the reduction of calculated half-widths.

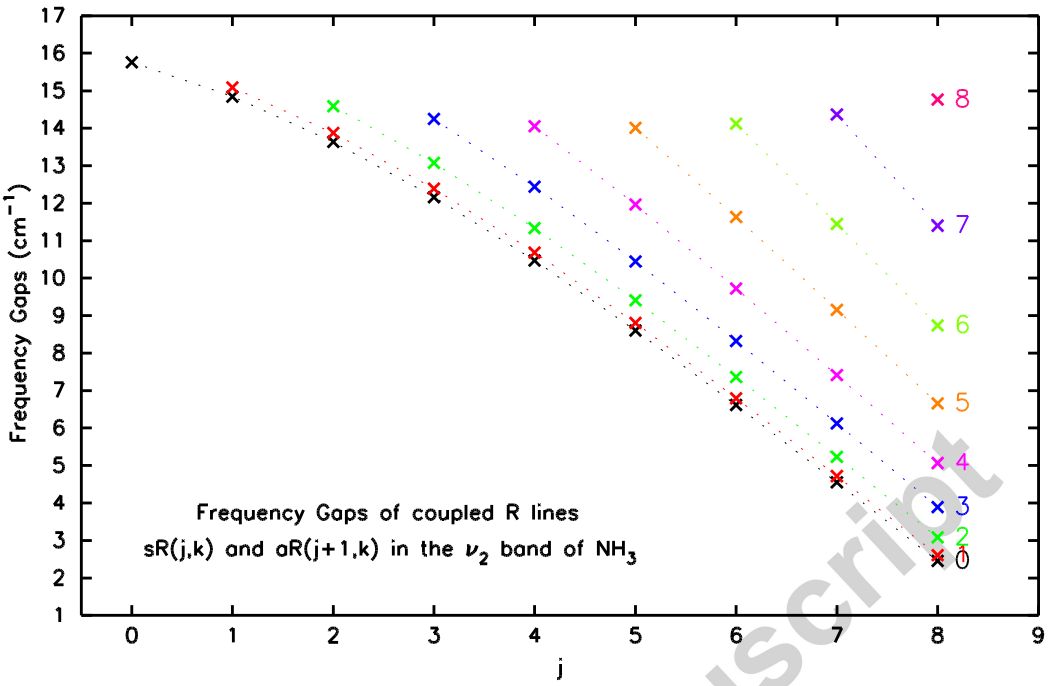

Fig. 8. Frequency gaps between sR(j,k) and aR(j+1,k) lines in the ν_2 band as a function of j and k.

4.4. Vibrational dependence of the half-widths

As mentioned above, the vibrational dependence of the half-widths is significant. This claim appears more clearly in Fig. 9 in which the half-widths of the sQ(j,j) lines for four vibrational parallel bands are plotted. The half-widths become smaller by a factor of 2.6 from the ν_1 band to the $2\nu_2 - \nu_2$ band, in good agreement with the experimental results. We note that for the $2\nu_2$ and $2\nu_2 - \nu_2$ bands, theoretical calculations are carried out without considering LC because its effects are negligible.

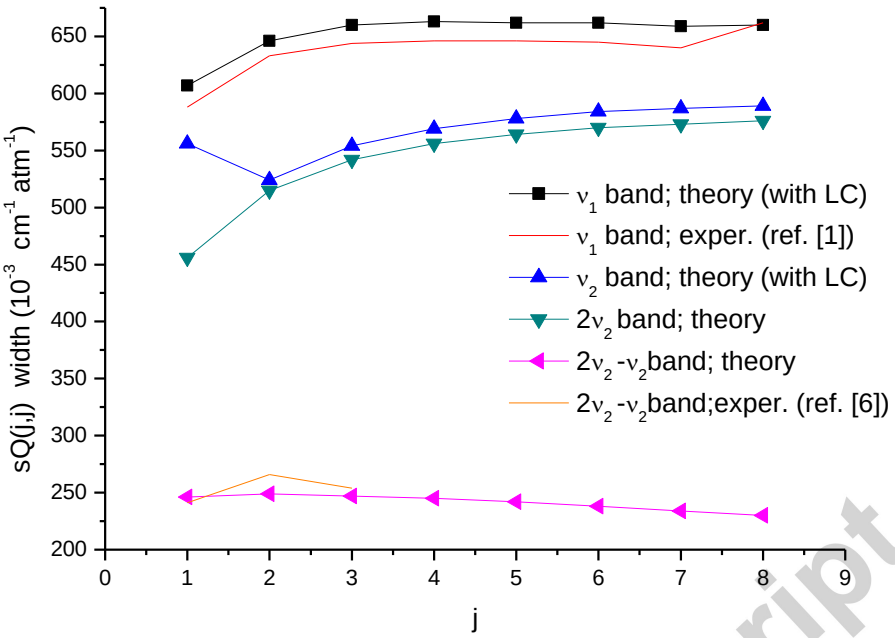

Fig. 9. Vibrational dependence of the widths of sQ(J,J) lines in four parallel bands of NH_3.

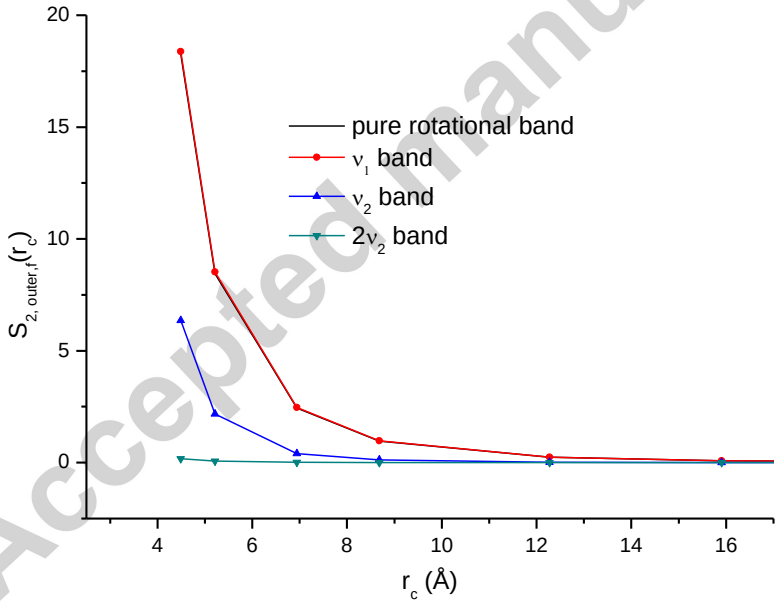

Fig. 10. The $S_{2,outer,f}$ term as a function of r_c for four different final vibrational levels. The line of interest is aR(3,3).

The half-width decrease shown in Fig. 9 results from the vibrational dependence of the matrix elements of $S_{2,outer,f}$. In Fig. 10, we present a plot of the $S_{2,outer,f}$ term associated with the aR(3,3) line as a function of r_c for the ground, ν_1, ν_2, and $2\nu_2$ bands. A minor part of the observed vibrational dependence is due to the different averaged dipole moments (cf. Table

1), but the latter cannot explain why, for instance, $S_{2,outer,f}$ practically vanishes as the band of interest varies from the ground state to the $2\nu_2$ level. Here again, the large ν_2 inversion splitting plays a major role. As is known, contributions to $S_{2,outer,f}$ mainly depend on the one dimensional (1-D) Fourier transform associated with V_{dd}, which is, in some sense, the analog of the resonance functions $f_n(k)$ of the ATC and RB theories. Both functions depend on a characteristic energy gap $\omega_{ff'} + \omega_{i_2 i_2'}$. It is worth mentioning here that now, f′ is a summation index and represents all possible choices of quantum numbers for states (i.e., the inversion symmetry s or a, the angular moment $j_{f'}$, and others) allowed by the potential components associated with the 1-D Fourier transforms.

It is well known that the magnitudes of the 1-D Fourier transforms decrease very quickly as their arguments increase beyond their center regions. In both the ground and ν_1 bands, because the inversion splitting is small, $\omega_{ff'}$ may be approximated by $B\left[j_f\left(j_f+1\right) - j_f'\left(j_f'+1\right)\right]$. Among all of the choices of $\omega_{ff'}$, some of them are small as well. This is the case of the dipole allowed ones $\Delta j_f = 0$, which lead, via the 1-D Fourier transform $F_{100100}\left(\omega_{ff'} + \omega_{i_2 i_2'}\right)$, to very significant contributions to $S_{2,outer,f}$. However, the above statement is not valid for the $\nu_2 = 1$ and $\nu_2 = 2$ modes because their inversion splitting values are not small. In this case, $\omega_{ff'}$ is given by $\pm\,\delta_{sa}^{\nu_2} + B\left[j_f\left(j_f+1\right) - j_f'\left(j_f'+1\right)\right]$, and for example, the choice of f′ with $\Delta j_f = 0$ are no more resonant. Except for some rare cases, the large splitting completely eliminates the contributions to $S_{2,outer,f}$ from $F_{100100}\left(\omega_{ff'} + \omega_{i_2 i_2'}\right)$.

With Fig. 10, one can easily understand the results presented in Fig. 9. In the ν_1 band (as in the pure rotational one), the contributions of $S_{2,outer,f}$ and $S_{2,outer,i}$ are almost identical. On the other hand, for the ν_2 and $2\nu_2$ bands the $S_{2,outer,f}$ term is much smaller than $S_{2,outer,i}$ so that the latter alone practically determines calculated half-widths. Things are even amplified in the $2\nu_2$ - ν_2 band where the blue curve (called ν_2) in Fig. 10 corresponds to $S_{2,outer,i}$ while the green one (called $2\nu_2$) corresponds to $S_{2,outer,f}$, leading to the observed "huge" decrease of the half-widths.

4.5. Broken approximate doublet symmetry

In paper I, we have explained why the partners of a doublet (i.e. sP(j,k) and aP(j,k)) in the ν_1 band have almost equal half-widths. However, as shown in Table 3, it is risky to extrapolate this approximate symmetry to other bands. Let us consider the doublet of s,aP(2,1) in the ν_2 band first. In this case the half-width γ_s is significantly larger than γ_a. Meanwhile, the opposite is true for s,aP(3,1). It turns out that the inversion splitting again is responsible for this symmetry breaking. Indeed, let us look at $\omega_{ff'}$, the key component of the characteristic energy gaps, appearing as the argument of $F_{100100}\left(\omega_{ff'} + \omega_{i_2 i_2'}\right)$ in the expression for $S_{2,outer,f}$. For the two partner transitions of 1 1 a ← 2 1 s (i.e., sP(2,1)) and 1 1 s ← 2 1 a (i.e., aP(2,1)), one has $j_f = 1$. The summation index f′ thus corresponds to $j_{f'}$ = 0, 1, and 2. But, simultaneously, the inversion symmetry must be "s" for sP(2,1) and "a" for

aP(2,1) because their final states have the "a" and "s" symmetries respectively, and the selection rule of inversion symmetry in F_{100100} requires a switch of s ↔ a. Corresponding to these possible j_f' values, the rotational energy change (in units of cm^{-1}) are $[E_{rot}(j_f) - E_{rot}(j_f')]$ = 20, 0, and −40 cm^{-1}. Thus, an almost perfect compensation in $\omega_{ff'}$ happens only for $j_f' = 2$ and a case of the doublet splitting equal to 36 cm^{-1}. The latter corresponds to an inversion energy change of $E_{inv}(a) - E_{inv}(s)$. Therefore, in order to have large contributions to $S_{2,outer,f}$, the final state of P(2,1) must have the "a" symmetry and this is just the line of sP(2,1).

The same argument is also applicable for the doublet of s,aP(3,1). In this case, $j_f = 2$ and $j_f' = 1$, 2, and 3 and the corresponding $E_{rot}(j_f) - E_{rot}(j_f') = 40$, 0, and −60 cm^{-1}, respectively. An almost perfect compensation happens only for $j_f' = 1$ and the doublet splitting change equals to −36 cm^{-1} resulting from $E_{inv}(s) - E_{inv}(a)$. This is just the line of aP(3,1).

Table 3 Broken symmetry of half-widths for some doublets (in units of 10^{-3} cm^{-1} atm^{-1})

Band	Doublet	γ_s	γ_a
ν_2	P(2,1)	471	359
ν_2	P(3,1)	326	422
$\nu_2 - 2\nu_2$	Q(1,1)	246	385
$\nu_2 - 2\nu_2$	Q(2,2)	250	197

Similarly, one can explain the broken symmetry observed in the $2\nu_2$ - ν_2 band. But here, it results from the $S_{2,outer,i}$ term. The reader can easily explain the results given in Table 3, because the $S_{2,outer,i}$ term of aQ(1,1) in this band is exactly the same as $S_{2,outer,f}$ of sP(2,1) in the ν_2 band. Similarly, the $S_{2,outer,i}$ term of sQ(2,2) is just the $S_{2,outer,f}$ term of aP(3,1).

Finally, we note that for higher j and k values, there are no more effective compensations happening between the inversion splitting and changes of rotational energy of the active molecule. As a result, the broken symmetry disappears and the approximate symmetry for the doublets components becomes valid again.

4.6. Comparison with HITRAN 2012

As already mentioned in paper I, for the ν_1 band the agreement between calculated (or experimental) widths and those stored in HITRAN 2012 [20] is poor in some cases. A similar conclusion is also valid for the ν_2 band as shown in Figs. 11 and 12. In our opinion, the database needs to be improved by taking into account both the rotational and vibrational dependences of the self-broadened widths.

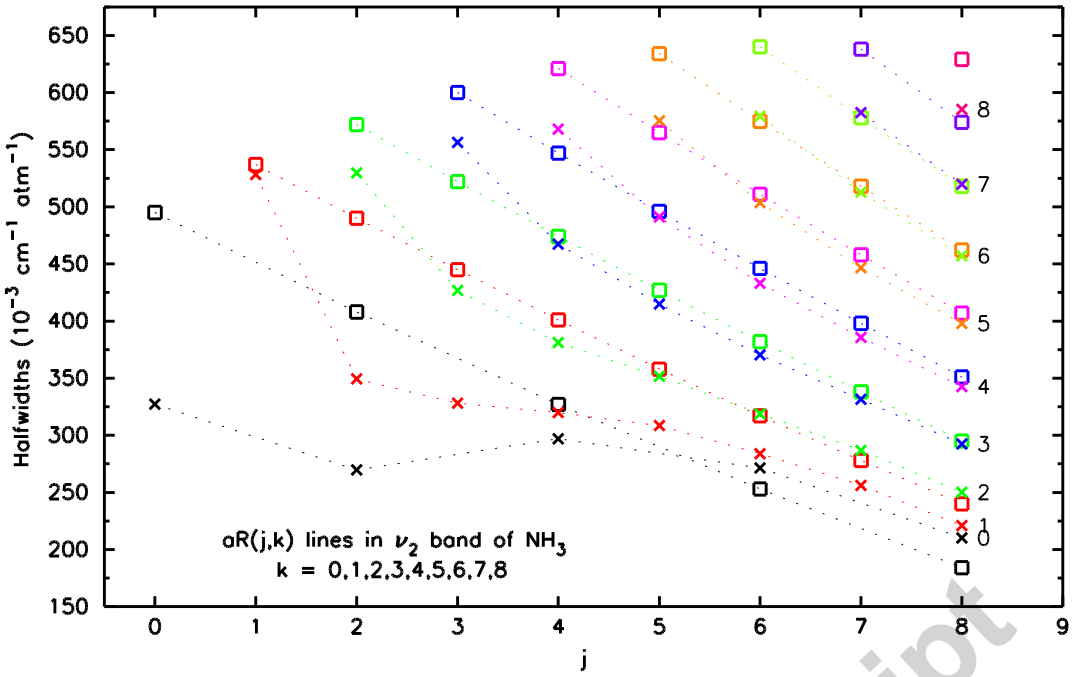

Fig. 11. Calculated half-widths of aR(j,k) lines (×) and HITRAN data (□) in the ν_2 band.

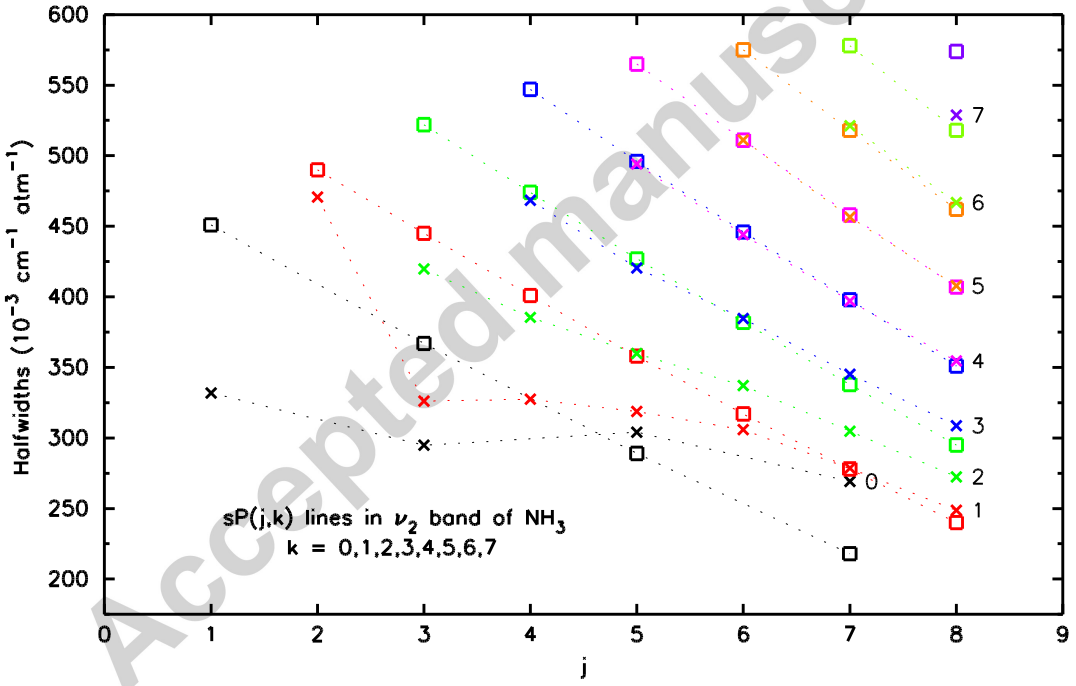

Fig. 12. Calculated half-widths of sP(j,k) lines (×) and HITRAN data (□) in the ν_2 band.

5. LINE MIXING EFFECTS

As known from previous studies, our formalism allows one to calculate the whole relaxation matrix. Then, with the method detailed in paper II, one can calculate the first order Rosenkranz mixing parameters [21]

$$Y_l = 2\sum_{n\neq l}\frac{d_n}{d_l}\,\frac{W_{n,l}}{\omega_l-\omega_n}. \qquad (6)$$

Because these parameters have been experimentally determined by Aroui et al. [11] for many lines in the ν_2 and $2\nu_2$ bands, it is worth to compare our theoretical predictions with their experimental data. Although the agreement between measured and calculated half-widths is good, a severe disagreement occurs for the Y_l parameters, as shown in Table 4 where some samples in the R(4,K) manifold are presented. In this case, the experimental results are higher than the calculated values by two orders of magnitude. Note that they are quite comparable to the values obtained in the ν_1 band although effects from LC dramatically differ from each other for these two bands (remember that we have obtained a rather good agreement between the experimental and theoretical LM signatures for the R(3,k) manifold in the ν_1 band). In addition, a similar problem also happens in the $2\nu_2$ band. In Table 5, we present measured Y_l values for some aQ(j,j) lines in the $2\nu_2$ band. For the calculated results which are not presented in Table 5, they are almost zero. As a reference, measured and calculated results in the ν_1 band are also listed. Given the fact that for the $2\nu_2$ band, almost no line couplings exist, how is it possible to observe such large mixing parameters comparable to those in the ν_1 band? Therefore, we strongly doubt the correctness of these measured results in the ν_2 and $2\nu_2$ bands.

Table 4 Rosenkranz parameters Y_l (in units of atm^{-1}) for the aR(4,k) manifold

k	Experiments Ref. [11] in the ν_2 band	Calculated values in the ν_2 band	Calculated values in the ν_1 band
0	0.29 (0.04)	3.9×10^{-3}	−1.2
1	−0.63 (0.08)	2.9×10^{-3}	0.04
2	0.35 (0.06)	1.5×10^{-3}	0.13
3	0.20 (0.03)	0.5×10^{-3}	0.23
4	0.32 (0.04)	~ 0.0	0.33

Table 5 Rosenkranz parameters Y_l (in units of atm^{-1}) for some aQ(j,j) lines

Line	Experiments Ref. [11] in the $2\nu_2$ band	Experiments Ref. [1] in the ν_1 band	Calculations Ref. [3] in the ν_1 band
aQ(2,2)	0.85 (0.16)	−0.41	0.28
aQ(3,3)	−1.48 (0.24)	0.57	0.34
aQ(4,4)	−2.48 (0.18)	0.52	0.37
aQ(5,5)	2.47 (0.23)	0.82	0.39
aQ(6,6)	−0.36 (0.07)	0.89	0.41

We have encountered a similar situation in our previous analysis of LC in the ν_1 band. While our calculated W matrix elements reproduced very well the observed line mixing effects in the Q branch, the calculated Y_l parameters strongly disagree with the measured ones. In our opinion, here too, the measured Y_l are "effective" parameters derived from a fitting procedure applied to "congested" spectra recorded in experimental conditions (too small NH_3 pressures, too long cell…) not favorable for an accurate determination of the

mixing parameters Y_l. In the following, we provide additional arguments supporting this assertion.

As shown in Sec. 4, with respect to the ν_1 band, the intra-doublet coupling is significantly weaker in the ν_2 band and becomes totally negligible in the $2\nu_2$ band. As a result, one should observe a very significant decrease of the corresponding off-diagonal matrix elements of W as the band of interest goes from ν_1 to ν_2. This is exactly what we observe in Tables 6 and 7. As expected from the above analysis of LC, very weak W matrix elements between adjacent (in j) components subsist, but due to the denominator in Eq. (6), they lead to small values of the Y_l parameters, in total contradiction with the experimental data of Ref. [11], which have amplitudes similar to those measured and calculated in the ν_1 band (and the same is true for the $2\nu_2$ band).

Table 6 The most efficient off-diagonal elements $W_{n,l}$ (in units of 10^{-3} cm^{-1} atm^{-1}) coupling one line denoted by l to others denoted by n

$l = aQ(3,3)$			$l = aR(3,3)$			$l = aR(4,4)$		
n	ν_1	ν_2	n	ν_1	ν_2	n	ν_1	ν_2
sQ(3,3)	−298	−1.3	sR(3,3)	−265	−1.3	sR(4,4)	−294	−1.3
sQ(4,3)	−22.5	−0.21	sR(4,3)	−5	−0.03	sR(5,4)	−5.2	~0
aQ(4,3)	−13.4	−0.6	aR(4,3)	−5.2	−0.22	aR(5,4)	−5.4	−0.2

Table 7 The most efficient off-diagonal elements $W_{n,l}$ (in units of 10^{-3} cm^{-1} atm^{-1}) coupling aR(4,3) to other lines denoted by *n*

$aR(4,3)$		
n	ν_1	ν_2
sR(3,3)	−7.5	−4.2
aR(3,3)	−5.2	−0.2
sR(4,3)	−202	−1.8
sR(5,3)	−6.5	~0
aR(5,3)	−6.2	−0.4

As mentioned above, we do think that the experimental Y_l of Ref. [11] are "effective" parameters due to strong correlations in the fitting process. In order to go further and clarify the situation, we suggest two experiments limited to some very specific spectral regions.

The first one is to investigate the aR(1,1) line which, as discussed in Sec. 4, coupled to sQ(1,1). Although the coupling is relatively weak, it nevertheless leads to a "significant" value of Y_l. Here, "significant" means that Y_l should be measureable if the experimental conditions are optimized. The NH_3 pressures should be sufficiently high to favor the mixing effect but sufficiently low such that the line remains well isolated from the others. From Fig. 13 it seems that an experiment with a very good signal to noise ratio, and using an "ad-hoc" cell length could anable the determination of Y_l and a meaningful comparison with the

calculated one. In this figure and the two following ones the first order correction is the difference between the Rozenkranz and Lorentzian profiles.

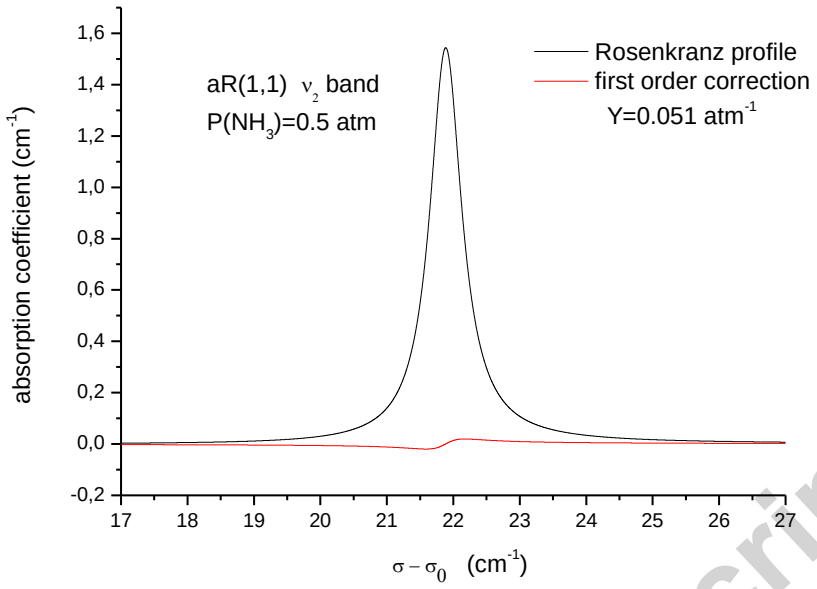

Fig. 13. Absorption coefficient of aR(1,1) in the ν_2 band at a sample pressure of 0.5 atm. ($\sigma_0 = 950\ cm^{-1}$).

Next, one can consider the aR(4,K) manifold in the region 1028 -1037 cm^{-1}. The experiment should enable to determine which set of Y_l is more reliable between our calculated results and those measured by Aroui et al. [11]. By looking at the high resolution spectrum reproduced in Ref. [22], it appears that this manifold is relatively isolated, only slightly "contaminated" by the presence of the sR(2,2) and sR(2,1) lines at moderate NH_3 pressures. Then, the measurement of the absorption coefficient at pressures of NH_3 around 0.6 atm should discriminate between the two sets of Y_l. The prediction based on the parameters of Ref. (11) is shown in Fig. 14, while that corresponding to our theoretical parameters is poltted in Fig. 15. Note that the first order correction derived from the theoretical Y_l is multiplied by 100 in Fig. 15. Given the fact that our theoretically calculated Y_l values are so small, it should be impossible to measure any significant effect from line mixing on this manifold. Our conclusion is in complete opposition with what would be expected from Aroui's Y_l values.

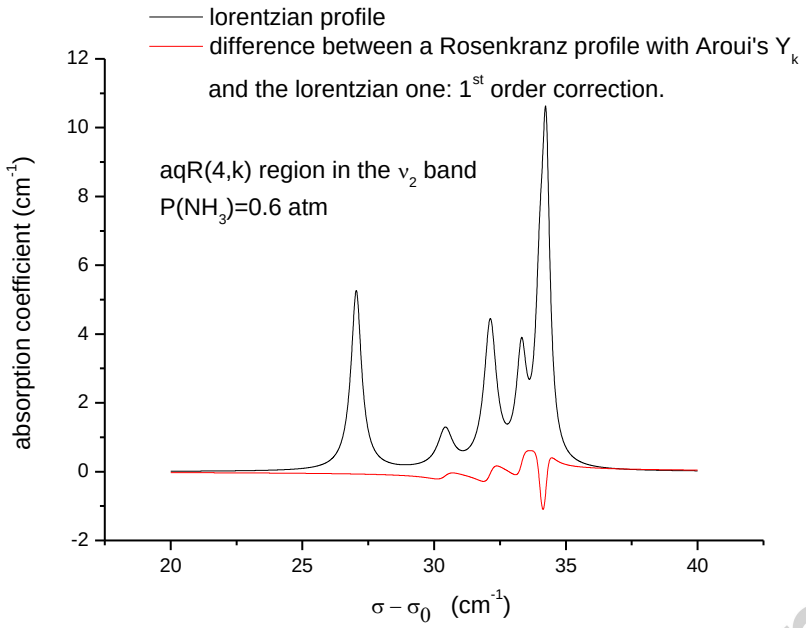

Fig. 14. Absorption coefficient of the aR(4,k) manifold in the ν_2 band at a sample pressure of 0.6 atm. The set of Y_l used is that measured in Ref. [11]. The line around 1027 cm^{-1} (located at 1027- σ_0) is due to the presence of sR(2,2) and sR(2,1) which slightly contaminate the manifold ($\sigma_0 = 1000\ cm^{-1}$).

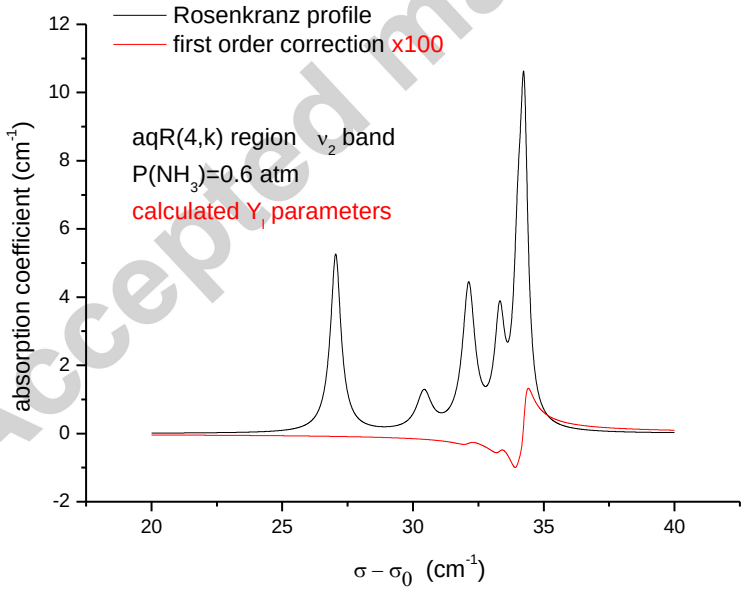

Fig. 15. Absorption coefficient of the aR(4,k) manifold in the ν_2 band at a sample pressure of 0.6 atm. The set of Y_l used is the theoretical one. Note that the first order correction has been multiplied by 100. ($\sigma_0 = 1000\ cm^{-1}$).

6. CONCLUSION

We have calculated relaxation matrices of self-broadened half widths of NH_3 lines in several parallel bands whose inversion splitting values change over a wide range. Detailed comparisons of the measured and calculated half-widths (i.e., diagonal elements of the W matrices) show a good agreement. The present work has provided a new insight on the role played by the inversion splitting (mainly due to a change of the ν_2 mode) on both the intra-doublet coupling and the vibrational dependence of the half-widths, through the 2-D Fourier transforms derived from components of the potential models adopted in the calculations.

As the ν_2 mode is excited, the intra-doublet coupling disappears and consequently, the corresponding off-diagonal element $W_{s,a}$ practically vanishes as well. This is in contrast with what have been observed in the ν_1 band. With respect to the Rosenkranz line mixing parameters, our calculated values in the ν_2 and $2\nu_2$ band are one to two orders smaller than those obtained for the ν_1 band. In comparison with measured values by Aroui et al. [11] for these two bands, their values are two orders of magnitude larger than ours. At present, the origin of this large discrepancy is unclear. In our opinion, it may be due to improper experimental conditions. It would be helpful if the measurements could be performed under more appropriate conditions. Two experiments for relatively well isolated manifolds, even at relatively "high" NH_3 densities, have been suggested by us. In our opinion, these measurements should provide more reliable values of Y_l and thus a more meaningful test of the theory.

It is worth mentioning that such "clean" measurements have already been reported for closely spaced pP(j,k) doublets in the ν_4 band [23]. This implies that it has been possible to measure the $W_{s,a}$ matrix elements as well as to determine their j and k dependences. On the other hand, in order to make a comparison, it becomes necessary to extend the present formalism to perpendicular bands. This work is currently being carried out by us and the results obtained are very encouraging. The summary of this work will be presented in a forthcoming paper.

Finally our formalism could be easily applied to the case of foreign gas broadening including rare gas perturbers for which many experimental results exist in the literature [1,23,24]. Some of them, especially the NH_3-rare gas broadening, have revealed LM features strongly differing from those observed in self-broadened lines. One of the possible explanation is the presence of potential components with $K_1 \neq 0$ which are absent in self-broadening. Since sophisticated potentials for some NH_3-rare gas atoms are available, they will give us the opportunity to test our semi-classical formalism with more general potential models.

ACKNOWLEDGEMENTS

The authors would like to thank Dr. Keeyoon Sung (JPL) for helpful discussions. We also thank the reviewers for greatly improving the manuscript. Two of the authors (Q. Ma and R. H. Tipping) acknowledge financial support from NSF under grant 1501297. This research used resources of the National Research Scientific Computing Center, which is supported by

the Office of Science of the U.S. Department of Energy under Contract No. DE-AC02-05CH11231.

REFERENCES

(1) Pine A.S, Markov V.N. Self and foreign gas broadened lineshapes in the ν_1 band of NH_3. J. Quant. Spectrosc. Radiat. Transfer 2004; 228: 121-142.

(2) Brown L.R, Peterson D.B. An empirical expression for linewidths of ammonia from far-infrared measurements. J. Mol. Spectrosc. 1994; 168: 593-606.

(3) Ma Q, Boulet C. The relaxation matrix for symmetric tops with inversion symmetry. I. Effects of line coupling on self-broadened ν_1 and pure rotational bands of NH_3. J. Chem. Phys. 2016; 144 (224303): 1-14.

(4) Boulet C, Ma Q. The relaxation matrix for symmetric tops with inversion symmetry. II. Line mixing effects in the ν_1 band of NH_3. J. Chem. Phys. 2016; 144 (224304): 1-9.

(5) Baldacchini G, Marchetti S, Montelatici V, Buffa G, Tarrini O. Experimental and theoretical investigation of self-broadening and self-shifting of ammonia transition lines in the ν_2 band. J. Chem. Phys. 1982; 76: 5271-5277.

(6) Baldacchini G, Marchetti S, Montelatici V, Sorge V, Buffa G, Tarrini O. Self-broadening and self-shifting of ammonia lines in the $2\nu_2$ band. J. Chem. Phys. 1983; 78: 665-668.

(7) Baldacchini G, Marchetti S, Montelatici V, Buffa G, Tarrini O. Self-broadening and self-shifting of ammonia lines in the $2\nu_2$ band around 16 μm. J. Chem. Phys. 1985; 83: 4975-4977.

(8) Tsao C.J, Curnutte B. Linewidths of pressure broadening spectral lines. J. Quant. Spectrosc. Radiat. Transfer 1962; 2: 41-91.

(9) Nemtchinov V, Sung K, Varanasi P. Measurements of line intensities and half-widths in the 10-μm bands of $^{14}NH_3$. J. Quant. Spectrosc. Radiat. Transfer 2004; 83: 243-265.

(10) Aroui H, Nouri S, Bouanich J-P. NH_3 self-broadening coefficients in the ν_2 and ν_4 bands and line intensities in the ν_2 band. J. Mol. Spectrosc. 2003; 220: 248-258.

(11) Aroui H, Laribi H, Orphal J, Chelin P. Self-broadening, self-shift and self-mixing in the ν_2, $2\nu_2$, and ν_4 bands of NH_3. J. Quant. Spectrosc. Radiat. Transfer 2009; 110: 2037-2059.

(12) Guinet M, Jeseck P, Mondelain D, Pepin I, Janssen C, Camy-Peyret C, Mandin J-Y. Absolute measurements of intensities, positions and self-broadening coefficients of R branch transitions in the ν_2 band of ammonia. J. Quant. Spectrosc. Radiat. Transfer 2011; 112: 1950-1960.

(13) Ma Q, Boulet C, Tipping R.H. Refinement of the RB formalism considering effects from the line coupling. J. Chem. Phys. 2013; 139(034305): 1-16.

(14) Robert D, Bonamy J. Short range force effects in semi-classical molecular line broadening calculations. J. Phys. 1979; 40: 923-943.

(15) Cherkasov M.R. Theory of relaxation parameters of the spectrum shape in the impact approximation - I: General consideration. J. Quant. Spectrosc. Radiat. Transfer 2014; 141: 73-88.

(16) Cherkasov M. R. Theory of relaxation parameters of the spectrum shape in the impact approximation – II: .Simplifications, application for $^{q}Q(J,K)$ doublets in the ν_1 band of NH_3 self-broadening. J. Quant. Spectrosc. Radiat. Transfer 2014; 141: 73-88.

(17) Marshall M.D, Izqi K.C, Muenter J.S. IR-Microwave double resonance studies of dipole moments in the ν_1 and ν_3 states of ammonia. J. Chem. Phys. 1997; 107: 1037-1044.

(18) Cottaz C, Kleiner I, Tarrago G, Brown L.R, Margolis J.S, Poynter R.L, Pichett H.M, Fouchet T, Drossart P, Lellouch E. Line positions and intensities in the $2\nu_2/\nu_4$ vibrational system of $^{14}NH_3$ near 5-7 μm. J. Mol. Spectrosc. 2000; 203: 285-309.

(19) Keeyoon Sung (JPL). Personal communication (2016).

(20) Rothman L.S et al. The HITRAN2012 spectroscopic database. J. Quant. Spectrosc. Radiat. Transfer 2013; 130: 4-50.

(21) Note that the sign in Eq. (3) of II is wrong. It has been corrected here.

(22) Urban S, Spirko V, Papousek D, McDowell R.S, Nereson N.G, Belov S.P, Gershtein L.I, Maslovskij A.V, Krupnov A.F, Curtis J, Rao K.N. Coriolis and l-type interactions in the ν_2, $2\nu_2$, and ν_4 states of $^{14}NH_3$. J. Mol. Spectrosc. 1980; 79: 455-495. See Fig. 1a.

(23) Hadded S, Aroui H, Orphal J, Bouanich J-P, Hartmann J-M. Line broadening and mixing in NH_3 inversion doublets perturbed by NH_3, He, Ar and H_2. J. Mol. Spectrosc. 2001; 210: 275-283.

(24) Hadded S, Thibault F, Flaud P-M, Aroui H, Hartmann J-M. Experimental and theoretical study of line mixing in NH_3 spectra. II. Effect of the perturber in infrared parallel bands. J. Chem. Phys. 2004; 120: 217-223.

Highlights

- New formalism is applied to calculate line shape parameters in parallel bands of NH_3.
- Theoretical results are compared with measurements in the ν_2, $2\nu_2$, and $2\nu_2$-ν_2 bands.
- Half-widths and line mixing parameters strongly depend on excitation of the ν_2 mode.